SLAC-PUB-7774
December 1997

B PHYSICS BEYOND THE STANDARD MODEL*

JoAnne L. Hewett

Stanford Linear Accelerator Center
Stanford CA 94309, USA

Abstract

The ability of present and future experiments to test the Standard Model in the B meson sector is described. We examine the loop effects of new interactions in flavor changing neutral current B decays and in $Z \to b\bar{b}$, concentrating on supersymmetry and the left-right symmetric model as specific examples of new physics scenarios. The procedure for performing a global fit to the Wilson coefficients which describe $b \to s$ transitions is outlined, and the results of such a fit from Monte Carlo generated data is compared to the predictions of our two sample new physics scenarios. A fit to the $Zb\bar{b}$ couplings from present data is also given.

Based on presentations given at the *Workshop on Physics Beyond the Standard Model: Beyond the Desert: Accelerator and Nonaccelerator Approaches*, Tegernsee, Germany, June 8-14, 1997; *20th Anniversary Symposium: Twenty Beautiful Years of Bottom Physics*, Chicago, IL, June 29 - July 2, 1997; and the *7th International Symposium on Heavy Flavor Physics*, Santa Barbara, CA, July 7-11, 1997.

*Work supported by the Department of Energy, Contract DE-AC03-76SF00515

B PHYSICS BEYOND THE STANDARD MODEL

J.L. HEWETT
Stanford Linear Accelerator Center, Stanford CA 94309, USA

The ability of present and future experiments to test the Standard Model in the B meson sector is described. We examine the loop effects of new interactions in flavor changing neutral current B decays and in $Z \to b\bar{b}$, concentrating on supersymmetry and the left-right symmetric model as specific examples of new physics scenarios. The procedure for performing a global fit to the Wilson coefficients which describe $b \to s$ transitions is outlined, and the results of such a fit from Monte Carlo generated data is compared to the predictions of our two sample new physics scenarios. A fit to the $Zb\bar{b}$ couplings from present data is also given.

1 Overview

The B-meson system promises to yield a fertile testing ground of the Standard Model (SM). The large data samples which will be acquired over the next decade at CESR, the Tevatron, HERA, the SLAC and KEK B-factories, as well as the LHC will furnish the means to probe the SM at an unprecedented level of precision. It is well-known[1] that precision measurements of low-energy processes can provide an insight to very high energy scales via the indirect effects of new interactions. As such, the B sector offers a complementary probe of new physics, and in some cases may yield constraints which surpass those from direct collider searches or exclude entire classes of models.

New physics may manifest itself in the B system in several ways, for example, inconsistencies with the SM may be found in measurements of (i) the unitarity triangle, (ii) rare decays, or (iii) precision electroweak measurements of the decay $Z \to b\bar{b}$. In the first case, the angles of the unitarity triangle, commonly denoted as α, β, and γ, may reveal the existence of new physics in three distinct manners:

- $\alpha + \beta + \gamma \neq \pi$,
- $\alpha + \beta + \gamma = \pi$, but the individual values of the angles are outside of their SM ranges,
- $\alpha + \beta + \gamma = \pi$, but the values of the angles are inconsistent with the measured sides of the triangle.

These potential deviations may originate from new interactions in tree-level B decays, or by the virtual effects of new physics in loop mediated processes (*e.g.*, $B_d^0 - \bar{B}_d^0$ mixing or penguin decays of the B), with or without the presence of

new phases. Since the scale of the new physics is expected to be large compared to M_W, it is anticipated that additional tree-level contributions to B decay are suppressed. Further consequences of new degrees of freedom in the unitarity triangle are discussed by Fleischer.[2]

Here, we concentrate on the loop effects of new interactions in flavor changing neutral current (FCNC) B decays and in $Z \to b\bar{b}$. We note that most classes of models which induce large effects in the FCNC decays also affect $B_d^0 - \bar{B}_d^0$ mixing, and that measurements of several different rare decays may elucidate the origin of new interactions. $b \to s$ transitions provide an excellent probe of new indirect effects as they only occur at loop level in the SM, and they have relatively large rates for loop processes due to the massive internal-top quark and the Cabbibo-Kobayashi-Maskawa (CKM) structure of the contributing penguin and box diagrams. Also, long distance effects are expected to play less of a role due to the heavy B mass, and hence rare processes are essentially short distance dominated.

2 The $Zb\bar{b}$ Vertex

The SM continues to provide an excellent description of precision electroweak data,[3] where the few (small) deviations may be attributed to normal statistical fluctuations and not neccessarily to new physics. In particular, the observables which characterize the $Zb\bar{b}$ couplings, the ratio $R_b = \Gamma(Z \to b\bar{b})/\Gamma(Z \to$ hadrons) and the forward-backward asymmetry parameter A_b, are now measured to be only $\sim (1.5 - 2)\sigma$ away from their SM expectations.[3,4] This is in contrast to only a couple of years ago when R_b was measured to be anomalously high, yielding hopeful indications of physics beyond the SM.[5] In fact, the $Zb\bar{b}$ vertex has long been recognized as being sensitive to new physics which may not affect the light fermion vertices, and now constrains the parameter space of some models.[1] A model independent fit to possible shifts in the left- and right-handed $Zb\bar{b}$ couplings is presented in Fig. 1. Writing these couplings as

$$\begin{aligned} g_L^b &= -\frac{1}{2} + \frac{1}{3}\sin^2\theta_w^b + \delta g_L^b\,, \\ g_R^b &= \frac{1}{3}\sin^2\theta_w^b + \delta g_R^b\,, \end{aligned} \tag{1}$$

where $\delta g_{L,R}^b$ represents the coupling shifts from their SM values, and $\sin^2\theta_w^b$ is the b-quark effective weak mixing angle, we use ZFITTER4.9 to calculate the SM predictions (taking $m_t = 175$ GeV, $\alpha_s = 0.118$, and $\alpha_{em}^{-1} = 128.896$) and perform a fit to the full SLC/LEP $Z \to b\bar{b}$ data set. Here we see that the data is well described by the SM, with a slight preference for a heavier Higgs.

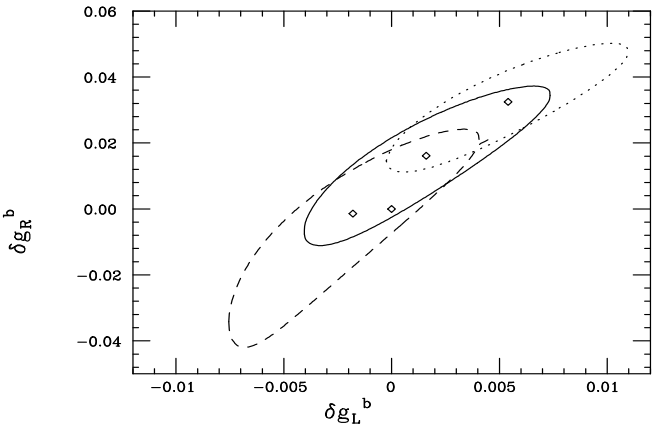

Figure 1: 95% C.L. fit to the parameters $\delta g^b_{L,R}$ using the full SLC/LEP $Z \to b\bar{b}$ data set and ZFITTER4.9 with $m_t = 175$ GeV. The dashed, solid, and dotted curves correspond to Higgs masses of 1 TeV, 300 GeV, and 65 GeV, respectively. The diamond at the center represents the SM, while the three other diamonds correspond to the location of the χ^2 minima for each Higgs mass. The values of the other input parameters are given in the text.

3 Formalism for $b \to s$ Transitions

The observation[6] of radiative penguin mediated processes, in both the exclusive $B \to K^*\gamma$ and inclusive $B \to X_s\gamma$ channels, has placed the study of rare B decays on a new footing and has provided powerful constraints on classes of models[7].

The effective field theory for $b \to s$ transitions is summarized at this meeting by Alf[8], however, we briefly review the features which are essential to the remainder of this talk. Incorporating the QCD corrections, these transitions are governed by the Hamiltonian

$$\mathcal{H}_{eff} = \frac{-4G_F}{\sqrt{2}} V_{tb}V_{ts}^* \sum_{i=1}^{10} C_i(\mu)\mathcal{O}_i(\mu)\,, \tag{2}$$

where the $\mathcal{O}_i$ are a complete set of renormalized operators of dimension six or less which mediate these transitions and are catalogued in, *e.g.*, Ref. [9]. The C_i represent the corresponding Wilson coefficients which are evaluated perturbatively at the electroweak scale, where the matching conditions are imposed, and then evolved down to the renormalization scale $\mu \approx m_b$. The

expressions for $C_i(M_W)$ in the SM are given by the Inami-Lim functions [10].

3.1 $B \to X_s \ell^+ \ell^-$ in the Standard Model

For $B \to X_s \ell^+ \ell^-$ this formalism leads to the physical decay amplitude (neglecting m_s and m_ℓ)

$$\begin{aligned} \mathcal{M} &= \frac{\sqrt{2} G_F \alpha}{\pi} V_{tb} V_{ts}^* \Big[C_9^{eff} \bar{s}_L \gamma_\mu b_L \bar{\ell} \gamma^\mu \ell + C_{10} \bar{s}_L \gamma_\mu b_L \bar{\ell} \gamma^\mu \gamma_5 \ell \\ &\quad - 2 C_7^{eff} m_b \bar{s}_L i \sigma_{\mu\nu} \frac{q^\nu}{q^2} b_R \bar{\ell} \gamma^\mu \ell \Big] , \end{aligned} \tag{3}$$

where q^2 represents the momentum transferred to the lepton pair. The next-to-leading order (NLO) analysis for this decay has been performed in Buras *et al.* [9], where it is stressed that a scheme independent result can only be obtained by including the leading and next-to-leading logarithmic corrections to $C_9(\mu)$ while retaining only the leading logarithms in the remaining Wilson coefficients. The leading residual scale dependence in $C_9(\mu)$ is cancelled by that contained in the matrix element of $\mathcal{O}_9$, yielding an effective value C_9^{eff}. In addition, the effective value for $C_7^{eff}(\mu)$ refers to the leading order scheme independent result, and we note that the operator $\mathcal{O}_{10}$ does not renormalize. The numerical estimates (in the naive dimensional regularization scheme) for these coefficients are displayed in Table 1. The reduced scale dependence of the NLO- versus the LO-corrected coefficients is reflected in the deviations $\Delta C_9(\mu) \lesssim \pm 10\%$ and $\Delta C_7^{eff}(\mu) \approx \pm 20\%$ as μ is varied. We find that the coefficients are much less sensitive to the remaining input parameters, with $\Delta C_9(\mu), \Delta C_7^{eff}(\mu) \lesssim 3\%$, varying $\alpha_s(M_Z) = 0.118 \pm 0.003$ [11], and $m_t^{phys} = 175 \pm 6\,\mathrm{GeV}$ [12]. The resulting inclusive branching fractions (which are computed by scaling the width for $B \to X_s \ell^+ \ell^-$ to that for B semi-leptonic decay) are found to be $(6.25^{+1.04}_{-0.93}) \times 10^{-6}$, $(5.73^{+0.75}_{-0.78}) \times 10^{-6}$, and $(3.24^{+0.44}_{-0.54}) \times 10^{-7}$ for $\ell = e, \mu$, and τ, respectively, taking into account the above input parameter ranges, as well as $B_{sl} \equiv B(B \to X \ell \nu) = (10.23 \pm 0.39)\%$ [13], and $m_c/m_b = 0.29 \pm 0.02$.

3.2 $B \to X_s \gamma$ in the Standard Model

The basis for the decay $B \to X_s \gamma$ contains the first eight operators in the effective Hamiltonian of Eq. (2). The next-to-leading order logarithmic QCD corrections have been recently completed, leading to a much reduced renormalization scale dependence in the branching fraction! The higher-order calculation involves several steps, requiring corrections to both C_7 and the matrix

Coefficient	$\mu = m_b/2$	$\mu = m_b$	$\mu = 2m_b$
C_7^{eff}	-0.371	-0.312	-0.278
C_9	4.52	4.21	3.81
C_{10}	-4.55	-4.55	-4.55

Table 1: Values of the Wilson coefficients for several choices of the renormalization scale. Here, we take $m_b = 4.87$ GeV, $m_t = 175$ GeV, and $\alpha_s(M_Z) = 0.118$.

element of $\mathcal{O}_7$. For the matrix element, this includes the QCD bremsstrahlung corrections [14] $b \to s\gamma + g$, and the NLO virtual corrections [15]. Summing these contributions to the matrix elements and expanding them around $\mu = m_b$, one arrives at the decay amplitude

$$\mathcal{M}(b \to s\gamma) = -\frac{4G_F V_{tb}V_{ts}^*}{\sqrt{2}} D \langle s\gamma|\mathcal{O}_7(m_b)|b\rangle_{tree}\,, \tag{4}$$

with

$$D = C_7(\mu) + \frac{\alpha_s(m_b)}{4\pi}\left(C_i^{(0)eff}(\mu)\gamma_{i7}^{(0)}\log\frac{m_b}{\mu} + C_i^{(0)eff} r_i\right)\,. \tag{5}$$

Here, the quantities $\gamma_{i7}^{(0)}$ are the entries of the effective leading order anomalous dimension matrix, and the r_i are computed in Greub *et al.* [15], for $i = 2, 7, 8$. The first term in Eq. (5), $C_7(\mu)$, must be computed at NLO precision, while it is consistent to use the leading order values of the other coefficients. For C_7 the NLO result entails the computation of the $\mathcal{O}(\alpha_s)$ terms in the matching conditions [16], and the renormalization group evolution of $C_7(\mu)$ must be computed using the $\mathcal{O}(\alpha_s^2)$ anomalous dimension matrix [17]. The numerical value of the branching fraction is then found to be (again, scaling to semi-leptonic decay)

$$B(B \to X_s\gamma) = (3.25 \pm 0.30 \pm 0.40) \times 10^{-4}\,, \tag{6}$$

where the first error corresponds to the combined uncertainty associated with the value of m_t and μ, and the second error represents the uncertainty from $\alpha_s(M_Z), B_{sl}$, and m_c/m_b. This is well within the range observed by CLEO[6] which is $B = (2.32 \pm 0.57 \pm 0.35) \times 10^{-4}$ with the 95% C.L. bounds of $1 \times 10^{-4} < B(B \to X_s\gamma) < 4.2 \times 10^{-4}$. We note that ALEPH has recently reported the preliminary observation of this inclusive decay, at a compatible rate [18].

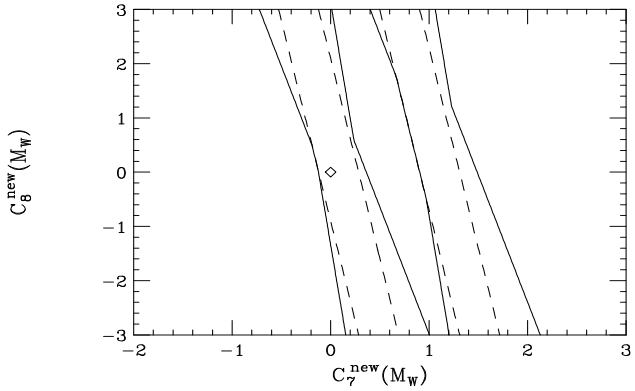

Figure 2: Bounds on the contributions from new physics to $C_{7,8}$. The region allowed by the CLEO data corresponds to the area inside the solid diagonal bands. The dashed bands represent the constraints when the renormalization scale is set to $\mu = m_b$. The diamond at the position (0,0) represents the Standard Model.

4 Model Independent Tests for New Physics in $b \to s$ Transitions

Measurements of $B(B \to X_s\gamma)$ constrain the magnitude, but not the sign, of $C_7(\mu)$. The coefficients at the matching scale ($\mu = M_W$) can be written in the form $C_i(M_W) = C_i^{SM}(M_W) + C_i^{new}(M_W)$, where $C_i^{new}(M_W)$ represents the contributions from new interactions. Due to operator mixing, $B \to X_s\gamma$ then limits the possible values for $C_i^{new}(M_W)$ for $i = 7, 8$. These bounds are summarized in Fig. 2. Here, the solid bands correspond to the constraints obtained from the current CLEO measurement, taking into account the variation of the renormalization scale $m_b/2 \leq \mu \leq 2m_b$, as well as the allowed ranges of the other input parameters. The dashed bands represent the constraints when the scale is fixed to $\mu = m_b$. We note that large values of $C_8^{new}(M_W)$ (which would yield an anomalous rate for $b \to sg$) are allowed even in the region where $C_7^{new}(M_W) \simeq 0$.

Measurement of the kinematic distributions[19,20] associated with the final state lepton pair in $B \to X_s\ell^+\ell^-$ as well as the rate for $B \to X_s\gamma$ allows the determination of the sign and magnitude of all the Wilson coefficients for the contributing operators in a model independent fashion. We have performed a Monte Carlo analysis in order to ascertain how much quantitative information will be obtainable at future B-Factories and follow the procedure outlined in Ref. [21]. For the process $B \to X_s\ell^+\ell^-$, we consider the lepton pair invariant mass distribution and forward-backward asymmetry[19] for $\ell = e, \mu, \tau$, and the tau polarization asymmetry[20] for $B \to X_s\tau^+\tau^-$. A three dimensional χ^2 fit to

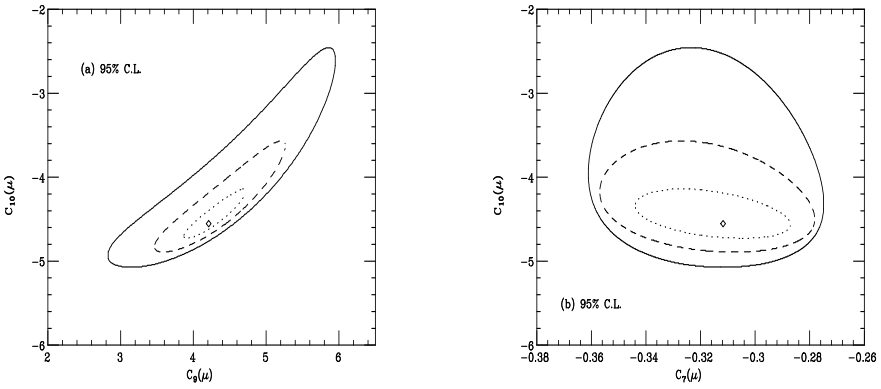

Figure 3: The 95% C.L. projections in the (a) $C_9 - C_{10}$ and (b) $C_7 - C_{10}$ planes, where the allowed regions lie inside of the contours. The solid, dashed, and dotted contours correspond to 3×10^7, 10^8, and 5×10^8 $B\bar{B}$ pairs. The central value of the SM prediction is labeled by the diamond.

the coefficients $C_{7,9,10}(\mu)$ is performed for three values of integrated luminosity, 3×10^7, 10^8, and 5×10^8 $B\bar{B}$ pairs, corresponding to the expected e^+e^- B-Factory luminosities of one year at design, one year at an upgraded accelerator, and the total accumulated luminosity at the end of these programs. The 95% C.L. allowed regions (including statistical errors only for $B \to X_s\ell^+\ell^-$ and a flat 10% error on $B \to X_s\gamma$) as projected onto the $C_9(\mu) - C_{10}(\mu)$ and $C_7(\mu) - C_{10}(\mu)$ planes are depicted in Figs. 3(a-b), where the diamond represents the central value for the expectations in the SM given in Table 1. We see that the determinations are relatively poor for 3×10^7 $B\bar{B}$ pairs and that higher statistics are required in order to focus on regions centered around the SM.

5 Supersymmetric Effects in $b \to s$ Transitions

These model independent bounds can be compared with model dependent predictions for the Wilson coefficients in order to ascertain at what level specific new interactions can be probed. First, we consider supersymmetric extensions to the SM. Supersymmetry (SUSY) contains many potential sources for flavor violation. For example, the flavor mixing angles among the squarks are *a priori* separate from the CKM angles of the SM quarks. We adopt the viewpoint here

that flavor-blind (diagonal) soft terms at the high scale are the phenomenological source for the soft scalar masses, and that the CKM angles are the only relevant flavor violating sources. The spectroscopy of the supersymmetric states is quite model dependent and we analyze two possibilities. The first is the familiar minimal supergravity model; in this instance all the supersymmetric states follow from a common scalar mass and a common gaugino mass at the high scale. The second case is where the condition of common scalar masses is relaxed and they are allowed to take on uncorrelated values at the low scale while still preserving gauge invariance.

We analyze the supersymmetric contributions to the Wilson coefficients [21,22] in terms of the quantities

$$R_i \equiv \frac{C_i^{susy}(M_W)}{C_i^{SM}(M_W)} - 1 \equiv \frac{C_i^{new}(M_W)}{C_i^{SM}(M_W)}\,, \tag{7}$$

where $C_i^{susy}(M_W)$ includes the full SM plus superpartner contributions. R_i is meant to indicate the fractional deviation from the SM value. We will search over the full parameter space of the minimal supergravity model, calculate the R_i for each generated point in the supersymmetric parameter space, and then compare with the expected ability of B Factories to measure the R_i as determined by our global fit to the Wilson coefficients. We generate [23] these supergravity models by applying common soft scalar and common gaugino masses at the boundary scale. The tri-scalar A terms are also input at the high scale and are universal. The radiative electroweak symmetry breaking conditions yield the B and μ^2 terms as output, with a sign(μ) ambiguity left over. (Here μ refers to the Higgsino mixing parameter.) We also choose $\tan\beta$ and restrict it to a range which will yield perturbative Yukawa couplings up to the GUT scale. We have generated thousands of solutions according to the above procedure. The ranges of our input parameters are $0 < m_0 < 500\,\mathrm{GeV}$, $50 < m_{1/2} < 250\,\mathrm{GeV}$, $-3 < A_0/m_0 < 3$, $2 < \tan\beta < 50$, and we have taken $m_t = 175\,\mathrm{GeV}$. Each supersymmetric solution is kept only if it is not in violation of present constraints from SLC/LEP and Tevatron direct sparticle production limits, and it is out of reach of LEP II. For each of these remaining solutions we now calculate R_{7-10}. Our results are shown in the scatter plots of Fig. 4 in the (a) $R_7 - R_8$ and (b) $R_9 - R_{10}$ planes. The diagonal bands represent the bounds on the Wilson coefficients as previously determined from our global fit. We see from Fig. 3(a) that the current CLEO data on $B \to X_s\gamma$ already place signigicant restrictions on the supersymmetric parameter space, whereas the minimal supergravity contributions to $R_{9,10}$ are predicted to be essentially unobservable.

A second, more phenomenological approach is now adopted. The maximal

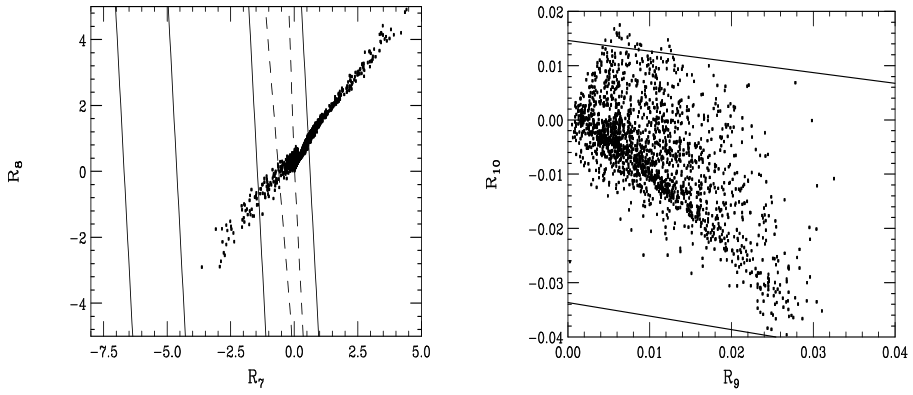

Figure 4: (a) Parameter space scatter plot of R_7 vs. R_8 in the minimal supergravity model. The allowed region from CLEO data lies inside the solid diagonal bands. The dashed band represents the potential future 10% measurement of $B \to X_s\gamma$ as described in the text. (b) Parameter space scatter plot of R_9 vs. R_{10}. The global fit to the coefficients obtained with 5×10^8 $B\bar{B}$ pairs corresponds to the region inside the diagonal bands.

effects for the parameters R_i can be estimated for a superparticle spectrum, independent of the high scale assumptions. However, we still maintain the assumption that CKM angles alone constitute the sole source of flavor violations in the full supersymmetric lagrangian. We will focus on the region $\tan\beta \lesssim 30$. The most important features which result in large contributions are a light $\tilde{t}_1$ state present in the SUSY spectrum and at least one light chargino state. For the dipole moment operators a light Higgsino state is also important. A pure higgsino and/or pure gaugino state have less of an effect than two mixed states when searching for maximal effects in R_9 and R_{10} and we have found that $M_2 \simeq 2\mu$ is optimal. Fig. 5 displays the maximum contribution to $R_{9,10}$ versus an applicable SUSY mass scale. The other sparticle masses which are not shown ($\tilde{t}_i$, $\tilde{l}_L$, etc.) are chosen to be just above the reach of LEP II or the Tevatron, whichever yields the best bound. We see that the maximum size of $R_{9,10}$ is somewhat larger than what was allowed in the minimal supergravity model, due to the lifted restriction on mass correlations.

Given the sensitivity of the observables it is instructive to narrow our focus to the coefficient of the magnetic dipole operator. The possibility exists that one eigenvalue of the stop-squark mass matrix might be much lighter than the other squarks, and we present results for $C_7(M_W)$ in the limit of one light squark, namely the $\tilde{t}_1$, and light charginos. We allow the $\tilde{t}_1$ to have arbitrary components of $\tilde{t}_L$ and $\tilde{t}_R$ since cross terms can become very

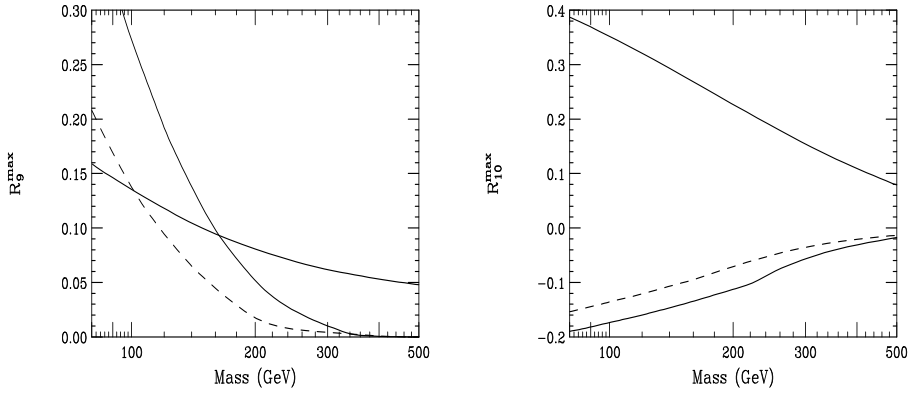

Figure 5: The maximum value of (a) R_9 and (b) R_{10} achievable for general supersymmetric models. The top solid line comes from the $t - H^{\pm}$ contribution and is displayed versus the $H^{\pm}$ mass. The bottom solid line is from the $\tilde{t}_i - \chi_j^{\pm}$ contribution with $\tan\beta = 1$ and is shown versus the $\chi_i^{\pm}$ mass. The dashed line is the $\tilde{t}_i - \chi_j^{\pm}$ contribution with $\tan\beta = 2$. The other mass parameters which are not plotted are chosen to be just above the reach of LEP II and the Tevatron.

important. This is especially noteworthy in the high $\tan\beta$ limit. We note that the total supersymmetric contribution to $C_7(M_W)$ will depend on several combinations of mixing angles in both the stop and chargino mixing matrices and cancellations can occur for different signs of μ[24]. The first case we examine is that where the lightest chargino is a pure Higgsino and the lightest stop is purely right-handed: $\chi_1^{\pm} \sim \tilde{H}^{\pm}$, $\tilde{t}_1 \sim \tilde{t}_R$. The resulting contribution to R_7 is shown as a function of the $\tilde{t}_R$ mass in Fig. 6 (dashed line) for the case of $m_{\chi_1^{\pm}} \gtrsim M_W$. Note that the SUSY contribution to $C_7(M_W)$ in this limit always adds constructively to that of the SM. Next we examine the limit where the light chargino is a pure Wino, this contribution is shown in Fig. 6 (dotted line). The effects of a light pure Wino are small since (i) it couples with gauge strength rather than the top Yukawa, and (ii) supersymmetric models do not generally yield a light $\tilde{t}_L$ necessary to couple with the Wino. Our third limiting case is that of a highly mixed $\tilde{t}_1$ state. We find that in this case large $\tan\beta$ solutions ($\tan\beta \gtrsim 40$) can yield greater than $\mathcal{O}(1)$ contributions to R_7 even for SUSY scales of 1 TeV! Low values of $\tan\beta$ can also exhibit significant enhancements; this is demonstrated for $\tan\beta = 2$ in Fig. 6 (solid line). We remark that large contributions are possible in this case in both negative and positive directions of R_7 depending on the sign of μ. We note that this is a region of SUSY parameter space which is highly motivated by $SO(10)$ grand

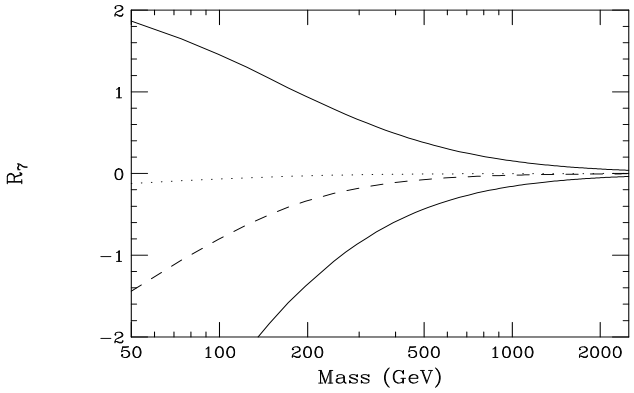

Figure 6: Contributions to R_7 in the different limits described in the text. The top solid line is the charged $H^{\pm}/t$ contribution versus $m_{H^{\pm}}$. The bottom solid line is the $\tilde{\chi}_1^{\pm}/\tilde{t}_1$ contribution versus $m_{\tilde{\chi}^{\pm}}$ where both the chargino and stop are maximally mixed states with $\mu < 0$. The dashed line is the $\tilde{H}^{\pm}/\tilde{t}_R$ contribution, and the dotted line represents the $\tilde{W}^{\pm}/\tilde{t}_1$ contribution. These two lines are both shown as a function of $\tilde{\chi}_1^{\pm}$ mass. All curves are for $\tan\beta = 2$ and $m_t = 175\,\mathrm{GeV}$.

unified theories.

Lastly, we compare the reach of rare B decays in probing SUSY parameter space with that of high energy colliders. We examine a set of five points in the minimal supergravity (SUGRA) parameter space that were chosen at Snowmass 1996 [25] for the study of supersymmetry at the NLC. Point #3 is the so-called "common" point used for a comparison of SUSY studies at the NLC, LHC, and Tev33. Once these points are chosen the sparticle mass spectrum is obtained, as usual, via the SUGRA relations and their contributions to $B \to X_s\gamma$ can be readily computed. The results are displayed in the $R_7 - R_8$ plane in Fig. 7 (labeled $1-5$ for each SUGRA point), along with the bounds previously obtained from our fits to the present CLEO data and to anticipated future data assuming the SM is realized. We see that four of the points should be discernable from the SM in future measurements, and that one of the points is already excluded by CLEO!

We thus conclude that rare B decays are indeed complementary to high energy colliders in searching for supersymmetry.

6 Left-Right Symmetric Model in $b \to s$ Transitions

The Left-Right Symmetric Model (LRM), which is based on the extended electroweak gauge group $SU(2)_L \times SU(2)_R \times U(1)$ can lead to interesting new

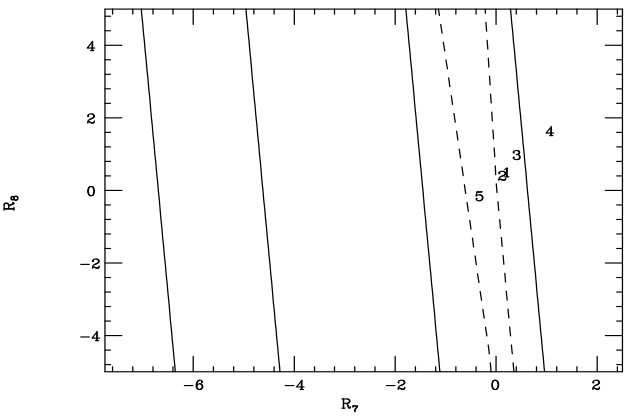

Figure 7: Values in the $R_7 - R_8$ plane for the five Snowmass NLC SUGRA points. The solid and dashed bands represent the present bounds from CLEO and those anticipated from future experiment, respectively, as described in Figure 3.

effects in the B system.[26,27] Due to the extended gauge structure there are both new neutral and charged gauge bosons, Z_R and W_R, as well as a right-handed gauge coupling, g_R, which is subject to the constraint $0.55 < \kappa \equiv g_R/g_L < 2.0$ from naturalness and GUT embedding conditions. The extended symmetry can be broken to the SM via the action of Higgs fields that transform either as doublets or triplets under $SU(2)_R$. This choice of Higgs representation determines both the mass relationship between the Z_R and the W_R (analogous to the condition that $\rho = 1$ in the SM) as well as the nature of neutrino masses. After complete symmetry breaking the charged W_R mixes with the SM W_L to form the mass eigenstates $W_{1,2}$ (where W_1 is the state which is directly produced at the Tevatron and LEP II). This mixing is described by two parameters: a real mixing angle ϕ and a phase α. In most models $\tan\phi$ is naturally of order of the ratio of masses $r = M_1^2/M_2^2$, or less, in the limit of large M_2. In this model the charged current interactions of the right-handed quarks are governed by a right-handed CKM matrix, V_R, which, in principle, need not be related to its left-handed counterpart V_L. V_R will then involve 3 new angles as well as 6 additional phases, all of which are *a priori* unknown parameters. Phenomenological constraints on the LRM are quite sensitive to variations of V_R. If one assumes manifest left-right symmetry, that is $V_R = V_L$ and $\kappa = 1$, then the $K_L - K_S$ mass difference implies that $M_R > 1.6$ TeV.

However, if that assumption is relaxed and V_R (as well as κ) is allowed to vary then W_R masses as low as 500 GeV can be accomodated by present data. This implies that the magnitude of $\tan\phi$ is $\leq few \times 10^{-2}$.

Clearly, this model contains many additional sources of CP violation; a partial cataloging of the possible effects can be found in Ref. [28]. In addition, the influence of the LRM may be felt in both tree and loop-level B decays. In particular, the possibility of a large right-handed component in the hadronic current describing $b \to c$ transitions has long been a subject of discussion[26]. Here we examine the possibility of using the rare decays $B \to X_s\gamma$ and $B \to X_s\ell^+\ell^-$ as a new tool in exploring the parameter space of the LRM. The exchange of a W_R within a penguin or box diagram, in analogy with the SM W_L exchange, can lead to significant deviations from the SM predictions for the rates and kinematic distributions in these decays.

In the LRM the complete operator basis governing $b \to s$ transitions in Eq. (2) must be expanded to

$$\mathcal{H}_{eff} = \frac{-4G_F}{\sqrt{2}} \sum_{i=1}^{12} C_{iL}(\mu)\mathcal{O}_{iL}(\mu) + L \to R\,. \tag{8}$$

This includes the right-handed counterparts to the usual 10 purely left-handed operators, as well as two pairs of additional four-quark operators of mixed chirality, $\mathcal{O}_{\infty\infty\mathcal{L}} \sim (\bar{s}_\alpha c_\beta)_R(\bar{c}_\beta b_\alpha)_L$ and $\mathcal{O}_{\infty\in\mathcal{L}} \sim (\bar{s}_\alpha c_\alpha)_R(\bar{c}_\beta b_\beta)_L$. The 2 subsets of left- and right-handed operators, $\mathcal{O}_{1-12L,R}$ are decoupled and do not mix under REG evolution. The decay $B \to X_s\gamma$, where the operators $\mathcal{O}_{1-8,11,12(L,R)}$ contribute, has been studied in some detail.[27] In particular it was shown that the left-right mixing terms associated with $\tan\phi \neq 0$ can be enhanced by a helicity flip factor of $\sim m_t/m_b$ and can lead to significantly different predictions from the SM even when $V_L = V_R$ and W_2 is heavy. This is depicted in Fig. 8 from Rizzo.[27] It is also clear from the figure that not only is the SM result is essentially obtained when $\tan\phi = 0$, but also that a conspiratorial solution occurs when $\tan\phi \simeq -0.02$. From the $B \to X_s\gamma$ perspective, these two cases are indistinguishable, independent of any further improvements in the measurement of the branching fraction.

LRM effects in $B \to X_s\ell^+\ell^-$ have recently been examined by Rizzo,[29] where it is found that the observables associated with this decay can distinguish the LRM from the SM. Here, all 24 operators in Eq. (8) participate in the renormalization and the matrix element now depends on $C_{7,9,10L,R}(\mu \sim m_b)$. The determination of the matching conditions at the electroweak scale for these 24 operators is tedious due to the large number of parameters, and in addition to new tree graphs, 116 one-loop diagrams must be evaluated. The predictions

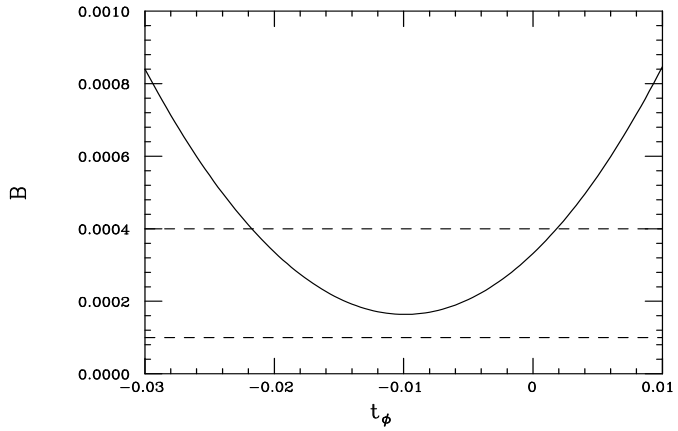

Figure 8: The $B \to X_s\gamma$ branching fraction in the LRM for $m_t(m_t) = 170$ GeV as a function of $\tan\phi$, assuming $\kappa = 1$, $V_R = V_L$, and $M_2 = 1.6$ TeV. The 95% C.L. CLEO results lie inside the dashed lines.

for the lepton pair mass distribution and forward-backward asymmetry for 4 sample points of the LRM parameter space is compared to the SM in Fig. 9. These 4 sample points yield the same rate the decay $B \to X_s\gamma$ as does the SM and satisfy all other low-energy constraints and direct Tevatron searches. As can be seen from this figure, these sample LRM predictions not only differ from the SM, but also from each other.

The extension of the operator basis in Eq. (8) implies that the conventional model independent determination of the Wilson coefficients discussed above will not apply in this case. In fact, this global fit technique has recently been shown to fail[29] for the LRM, and in doing so it provides a powerful probe for the existence of new operators. In general, there are three ways new physics can affect the global fit to the coefficients: (*i*) the numerical values for the coefficients are found to agree with SM expectations with a good χ^2; in this case the new physics is decoupled. (*ii*) A quality fit is obtained, but the fit values of the coefficients deviate from SM expectations. (*iii*) The χ^2 value for the best three parameter fit is found to be very large and cannot be explained by an under estimation of systematic uncertainties. It is this latter case which indicates the existence of additional operators. For the 4 LRM sample points discussed above, the 3 parameter ($C_{7,9,10L}$) global fit yields enormous values of $\chi^2/d.o.f.$, of order 1000/25, for a data sample of 5×10^8

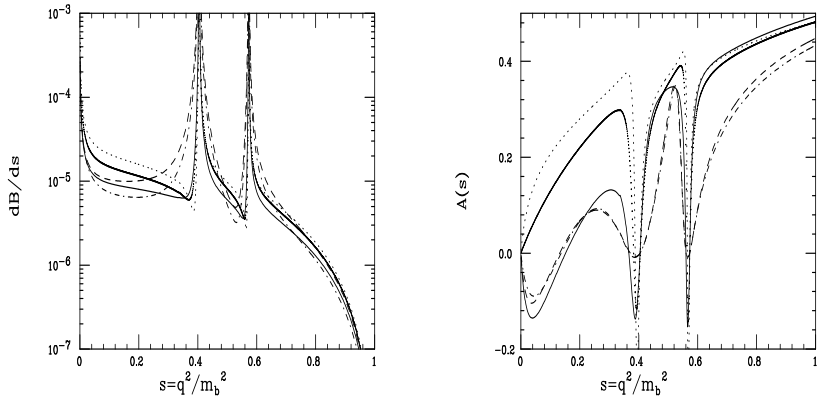

Figure 9: Differential decay distribution and lepton forward-backward asymmetry for the decay $B \to X_s \ell^+ \ell^-$ in the SM (solid) and for four points in the LRM parameter space which yield the SM value for $B(B \to X_s \gamma)$ and satisfy all other existing experimental constraints.

$B\bar{B}$ pairs, clearly signaling an inconsistent fit. For smaller data samples, *i.e.*, 5×10^7 $B\bar{B}$ pairs, the results are more dependent on the particular values of the LRM parameters. However, with sufficient statistics, it will be possible to observe the case where the canonical three coefficient fit fails, revealing not only the existence of physics beyond the SM, but that this new physics requires an extension of the operator basis.

7 Conclusions

This talk focused on supersymmetric and left-right symmetric model effects, as well as model independent tests for new physics, in rare B decays. Of course, there are numerous other candidates for physics models beyond the SM, as well as many other reactions where they can be tested. A brief compendium of these is given in Table 2. Here, we display the effects of (*i*) Multi-Higgs-Doublet Models (MHDM), with and without Natural Flavor Conservation (NFC), (*ii*) the Minimal Supersymmetric Standard Model (MSSM), and the supersymmetric models with squark alignment, effective SUSY scales, and R-parity violation, (*iii*) the LRM, with and without manifest left-right symmetry in the quark mixing matrices, (*iv*) a fourth generation, and (*v*) models with Z-boson mediated FCNC. We describe whether these models have the potential to cause large deviations from SM predictions in rare decays and $D^0 - \bar{D}^0$

Model	Rare Decays	$\frac{\Delta M_s}{\Delta M_d}$	New Phase B_d Mixing	$D^0 - \bar{D}^0$ Mixing
MHDM: with NFC	$B \to X_s\gamma$	= SM	No	Small
: no NFC	Not Really	$\neq$ SM	Yes	Big
MSSM	$B \to X_s\gamma$	= SM	No	Small
Squark Alignment	Small	$\sim$ SM	No	Huge
Effective SUSY	Small	$\sim$ SM	Yes	Small
R-Parity Violation	Big	$\neq$ SM	Yes	Big
LRM: $V_L = V_R$	$B \to X_s\gamma$ and	= SM	No	Small
: $V_L \neq V_R$	$B \to X_s\ell^+\ell^-$	$\neq$ SM	Yes	Big
4th Generation	Big	$\neq$ SM	Yes	Huge
Z-mediated FCNC	Big	$\neq$ SM	Yes	Big

Table 2: Model dependent effects of new physics in various processes.

mixing, whether new phases exist which contribute to $B_D^0 - \bar{B}_d^0$ mixing, and whether the new physics effects cancel in the ratio of mass differences in the B_s to B_d systems. This table is only intended to give a quick indication of potential effects.

In conclusion, we see that the B sector can provide a powerful probe, not only for the existence, but also for the structure of physics beyond the SM.

1. For a review, see, J.L. Hewett, T. Takeuchi, and S. Thomas, in *Electroweak Symmetry Breaking and New Physics at the TeV Scale*, ed. T. Barklow *et al.* (World Scientific, Singapore 1996).
2. R. Fleischer, these proceedings.
3. The LEP Collaborations, the LEP Electroweak Working Group, and the SLD Heavy Flavor Group, Report CERN-PPE/97-154 (1997).
4. S. Wagner, these proceedings.
5. See the talk given by K. Hagiwara at the *17th International Symposium on Lepton-Photon Interactions*, Beijing, China, August 1995, hep-ph/9512425.
6. CLEO Collaboration, M.S. Alam *et al.*, *Phys. Rev. Lett.* **74**, 2885 (1995); CLEO Collaboration, R. Ammar *et al.*, *Phys. Rev. Lett.* **71**, 674

(1993). For an update, see, T. Skwarnicki, these proceedings.
7. J.L. Hewett, in Proceedings of the *XXI Summer Institute on Particle Physics: Spin Structure in High Energy Processes*, Stanford, CA, 1993, ed. L. DePorcel and C. Dunwoodie, hep-ph/9406302.
8. A. Ali, these proceedings.
9. A.J. Buras and M. Münz, *Phys. Rev.* **D52**, 186 (1995).
10. T. Inami and C.S. Lim, Prog. Theor. Phys. **65**, 297 (1981).
11. R.M. Barnett *et al.*, (Particle Data Group), *Phys. Rev.* **D54**, 1 (1996).
12. P. Giromini, talk presented at *XVIII International Symposium on Lepton Photon Interactions*, Hamburg, Germany, 1997.
13. J. Richman, Proceedings of the *28th International Conference on High Energy Physics*, Warsaw, Poland, 1996, ed. Z. Ajduk and A.K. Wroblewski, hep-ex/9701014.
14. A. Ali and C. Greub, *Z. Phys.* **C49**, 431 (1991); *Phys. Lett.* **B259**, 182 (1991); *Phys. Lett.* **B361**, 146 (1995); N. Pott, *Phys. Rev.* **D54**, 938 (1996).
15. C. Greub, T. Hurth, and D. Wyler, *Phys. Lett.* **B380**, 385 (1996); *Phys. Rev.* **D54**, 3350 (1996).
16. K. Adel and Y.-P. Yao, *Phys. Rev.* **D49**, 4945 (1994).
17. K.G. Chetyrkin, M. Misiak, and M. Münz, *Phys. Lett.* **B400**, 206 (1997).
18. T. Skwarnicki, talk presented at *7th International Symposium on Heavy Flavor Physics*, Santa Barbara, CA, 1997.
19. A. Ali, T. Mannel, and T. Morozumi, *Phys. Lett.* **B273**, 505 (1991); A. Ali, G. F. Giudice, and T. Mannel, *Z. Phys.* **C67**, 417 (1995).
20. J.L. Hewett, *Phys. Rev.* **D53**, 4964 (1996).
21. J.L. Hewett and J.D. Wells, *Phys. Rev.* **D55**, 5549 (1997).
22. S. Bertolini *et al.*, *Nucl. Phys.* **B353**, 591 (1991); F. Borzumati, *Z. Phys.* **C63**, 291 (1994); F. Gabbiani *et al.*, *Nucl. Phys.* **B477**, 321 (1996); V. Barger *et al.*, *Phys. Rev.* **D51**, 2438 (1995); D. Choudhury *et al.*, *Phys. Lett.* **B342**, 180 (1995); J. Lopez *et al.*, *Phys. Rev.* **D51**, 147 (1995); R. Barbieri, G. Giudice, *Phys. Lett.* **B309**, 86 (1993); P. Cho, M. Misiak, and D. Wyler, *Phys. Rev.* **D54**, 3329 (1996); H. Baer and M. Brhlik, *Phys. Rev.* **D55**, 3201 (1997); T. Goto *et al.*, *Phys. Rev.* **D55**, 4273 (1997).
23. For description of the procedure we follow, see G. L. Kane, C. Kolda, L. Roszkowski, J. Wells, *Phys. Rev.* **D49**, 6173 (1994).
24. R. Garisto, and J. Ng, *Phys. Lett.* **B315**, 372 (1993).
25. M.N. Danielson *et al.*, Proceedings of *New Directions for High-Energy Physics*, Snowmass, CO, 1996, ed. D.G. Cassel *et al.*.
26. M.B. Voloshin, hep-ph/9704278; M. Gronau and S. Wakaizumi, *Phys.*

Rev. Lett. **68**, 1814 (1992).
27. D. Cocolicchio *et al.*, *Phys. Rev.* **D40**, 1477 (1989); G.M. Asatryan and A.N. Ioannisyan, Yad. Fiz. **51**, 1350 (1990); K.S. Babu, K. Fujikawa, and A. Yamada, *Phys. Lett.* **B333**, 196 (1994); P. Cho and M. Misiak, *Phys. Rev.* **D49**, 5894 (1994); T.G. Rizzo, *Phys. Rev.* **D50**, 3303 (1994); G. Bhattacharyya and A. Raychaudhuri, *Phys. Lett.* **B357**, 119 (1995); T.G. Rizzo, hep-ph/9705209.
28. T. Kurimoto, A. Tomita, and S. Wakaizumi, *Phys. Lett.* **B381**, 470 (1996); Y. Grossman, Y. Nir, and R. Rattazzi, hep-ph/9701231.
29. T.G. Rizzo, SLAC-PUB-7702, hep-ph/9802401.